

Combining multi-source information for crop monitoring

Mahmoud El Hajj
Cemagref, UMR TETIS
Montpellier, F-34093 France
mahmoud.elhajj@teledetection.fr

Serge Guillaume
Cemagref, UMR ITAP
Montpellier, F-34196 France
serge.guillaume@montpellier.cemagref.fr

Agnès Bégué
CIRAD, UMR TETIS
Montpellier, F-34093 France
agnes.begue@teledetection.fr

Jean-François Martiné
CIRAD, UR SCA
Saint-Denis, La Reunion, F- 97408 France
jean-francois.martine@cirad.fr

Abstract – Time series of optical satellite images acquired at high spatial resolution constitute an important source of information for crop monitoring, in particular for keeping track of crop harvest. However, the quantity of information extracted from this source is often restricted by acquisition gaps and uncertainty of radiometric values. This paper presents a novel approach that addresses this issue by combining time series of satellite images with other information from crop modeling and expert knowledge. An application for sugarcane harvest detection on Reunion Island using a SPOT5 time series is detailed. In a fuzzy framework, an expert system was designed and developed to combine multi-source information and to make decisions. This expert system was assessed for two sugarcane farms. Results obtained were in substantial agreement with ground truth data; the overall accuracy reached 96.07%.

Keywords: Remote sensing, time series, SPOT5, fusion, crop modeling, expert knowledge, cropping system, sugarcane, expert system.

1 Introduction

Over the past decade, time series of satellite images acquired at high spatial resolution have proven to be an important source of information for different agricultural applications. Several authors have recognized the benefits of this kind of data for monitoring agricultural lands [1], classifying land cover [2-4], mapping seasonal patterns and crop rotations [5, 6], and for many other uses (see papers collected in [7, 8]).

Nevertheless, the quantity of information extracted from time series of optical images is often restricted by several factors: acquisition gaps, atmospheric conditions, imperfect radiometric normalization, radiometric confusion, etc. Therefore, to make credible decisions, this information needs to be supplemented with data from other sources.

Few studies have combined high spatial resolution multi-temporal images and/or its derived products with ancillary data. Lucas et al. [9] evaluated the use of the Landsat ETM+ time series for mapping semi-natural habitats and

agricultural land cover by integrating topographic maps, digital elevation data, digital ortho-photography, field boundaries, and other supportive data. Metternicht et al. [10] mapped salinity distributions using an approach that integrated multi-temporal classification of Landsat TM images, physical and chemical soil properties, and landform attributes. Other studies have combined products derived from multi-temporal images to improve change detection performance when evaluating forest logging surfaces and when dealing with soil coverage during winter [11].

Until now, the integration of agronomic models with remote sensing data was restricted to model adjustment issues (assimilation, forcing, etc.) [12]. Little attention has been paid to the use of agronomical model outputs as an information source for supplementing remote sensing data. This kind of model, which is based on climatic and soil biophysical parameters, may provide useful information that can compensate for the lack of radiometric data.

Another source of substantial agricultural application information is expert knowledge.

Accordingly, the aim of this study is to present a novel approach for crop monitoring using time series of satellite images combined with information from crop modeling and expert knowledge. To describe this approach, an application for sugarcane harvest detection is detailed.

2 Study site and data sets

The study site consists of two sugarcane farms located in the north-east part of Reunion Island (Figure 1), which is a small territory of ~2,500 km² in the Indian Ocean (21°7' to 19°40' S, 55°13' to 61°13' E), where sugarcane is the main crop. The first farm is at an average altitude of 70 m and includes 33 fields with an average size of 5.4 ha. The second farm is at an altitude ranging from 400 to 700 m, and has 46 fields with an average size of 3.5 ha. As the study area is located in a tropical zone, the year is divided into two seasons: a hot rainy season from November to April, and a cool dry season from May to October.

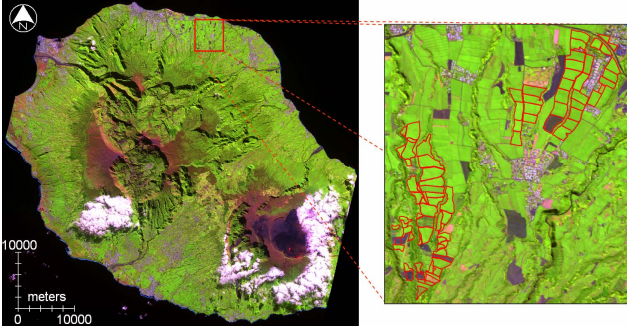


Figure 1. On the left, a false color composite (Red: band-4; Green: band-3; Blue: band-1) of a SPOT5 image acquired over Reunion Island. On the right, a close-up of the study site with sugarcane fields in red.

The satellite data set used in this study consists of 10 SPOT5 images acquired over Reunion Island between January 10th, 2003 and December 7th, 2004. Both SPOT5 instruments (HRG1 and HRG2) acquire radiation in four spectral bands with high spatial resolution: 10 m for the Green, Red, and Near Infra-Red (NIR) bands, and 20 m for the Short Wave Infra-Red (SWIR) band. The images belong to the KALIDEOS-ISLE REUNION database set up by the CNES¹ [13, 14]. All images were ortho-rectified and co-registered to the UTM coordinate system (zone 40 South) with a root mean square error of less than 0.5 pixel per image.

The radiometry of the images was corrected so that pixel values represent the top of canopy reflectances in the four spectral bands [15, 16]. Cloud mask was available for each image. Table 1 shows the characteristics of the images in the time series.

Block parcel boundaries for all Reunion Island were provided by the DDAF² and were refined by the CIRAD³ to define the boundaries of each field in the study site.

Daily climatic data recorded at La Mare meteorological station near the two sugarcane farms were collected for the period covered by the satellite time series. These data are daily estimations of rainfall (mm), potential evapotranspiration (mm), global radiation (J/m²), and minimum, maximum and mean temperature values (°C). Climatic data were required to run the crop growth model. A ground truth database was built by using harvest dates reported by farmers for each field during the 2003 and 2004 harvest campaigns. This database indicates the status of each field (whether it was harvested or not) between each pair of consecutive satellite acquisition dates in the time series.

Table 1. Characteristics of the SPOT5 time series.

Dates	SPOT5 Instrument	Incidence angle (in degree) (Right = -)	Solar elevation (in degree)	Phase angle (in degree)
01/10/2003	HRG 2	-04.65	64.10	21.28
05/04/2003	HRG 1	10.90	46.80	47.99
07/21/2003	HRG 1	10.58	41.20	53.13
09/01/2003	HRG 1	-04.42	50.63	37.31
12/19/2003	HRG 1	-02.90	67.20	19.90
04/11/2004	HRG 1	+17.95	52.45	48.41
06/18/2004	HRG 2	+03.25	39.10	51.95
08/19/2004	HRG 1	+17.96	48.50	51.24
11/06/2004	HRG 1	-19.16	66.63	09.07
12/07/2004	HRG 1	-12.28	66.65	11.19

3 Information from the time series

Using the time series of satellite images acquired at high spatial resolution, temporal profiles of NDVI (Normalized Difference Vegetation Index) can be extracted for each agricultural field. The NDVI is computed using reflectances (ρ) in the red and NIR bands:

$$NDVI = \frac{\rho_{NIR} - \rho_{red}}{\rho_{NIR} + \rho_{red}} \quad (1)$$

The temporal profile of NDVI provides useful information about the actual field status, and about its different historical stages. In general, this profile can be divided into two periods: a period in which NDVI values increase, corresponding to the vegetative development of the field crop, and another period with steady or decreasing values, corresponding to the maturation phase. Figure 2 shows an example of the temporal profile of a sugarcane field NDVI, extracted from a time series of SPOT images acquired with high temporal repeatability.

Using SPOT5 images in the time series and field boundaries, the temporal profile of NDVI was extracted for each field in the study site. This calculation was done after discarding cloud pixels using the cloud masks.

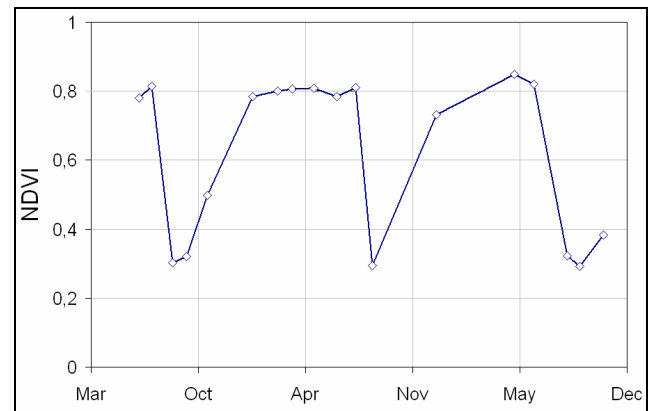


Figure 2. Example of the temporal profile of sugarcane NDVI calculated for a ratoon crop.

¹ Centre National d'Etudes Spatiales ; French Spatial Agency.

² Direction Départementale de l'Agriculture et de la Forêt ; Departmental Directorate of Agriculture and Forestry.

³ Centre de coopération Internationale en Recherche Agronomique pour le Développement ; French Agricultural Research Centre for International Development.

4 Information from crop modeling and expert knowledge

Since NDVI temporal profiles extracted from time series are often incomplete because of image acquisition gaps, atmospheric conditions and/or radiometric problems, other sources of information are required to reliably analyze these profiles in order to make good decisions.

4.1 Crop modeling

One way to meet this requirement is to simulate NDVI values using ancillary data. This can be done using crop growth models that generally provide estimates of LAI (Leaf Area Index) values by using climatic data and soil characteristics parameters. LAI estimations can then be transformed into NDVI values using relationships that are specific to the studied crop [17].

In our application, we used the sugarcane ecophysiological growth model MOSICAS [18] to simulate LAI temporal profiles at the field scale. This dynamic model estimates sugarcane growth on a daily time scale. It deals with biophysical data on the environment of the sugarcane field and the crop management sequence. Daily climatic data available in the dataset were used and soil characteristic parameters were obtained from the model code.

Since our aim was to acquire information based on NDVI, we transformed daily estimates of LAI made by MOSICAS to daily NDVI estimates using the regression model we proposed in [19] (Eq. 2):

$$NDVI = 1/9.713 * \ln(LAI/0.003) \quad (2)$$

From the simulated NDVI temporal profiles, we built a helpful indicator for harvest detection: T_n that represents the nominal time required (in days) to reach a given threshold of NDVI starting with a given harvest date.

Figure 3 illustrates an example of the relationship between the supposed harvest date and T_n for different NDVI threshold values. We observed that for high NDVI thresholds (0.7 in our example) the model was very sensitive to variations in climatic variables such as rainfall amount.

The information extracted from crop growth modeling (T_n), mainly based on climatic data, is independent from the time series of satellite images, and may suggest the possibility of sugarcane being harvested between two specific dates.

4.2 Expert knowledge

Knowledge about the phenological stages of the studied crop, as well as about cropping systems is key information that must be taken into account. This source allows a better understanding of the relationship between the temporal behavior of NDVI and the crop field status, and it offers important temporal constraints that particularly help in making decisions when there is a lack of radiometric data.

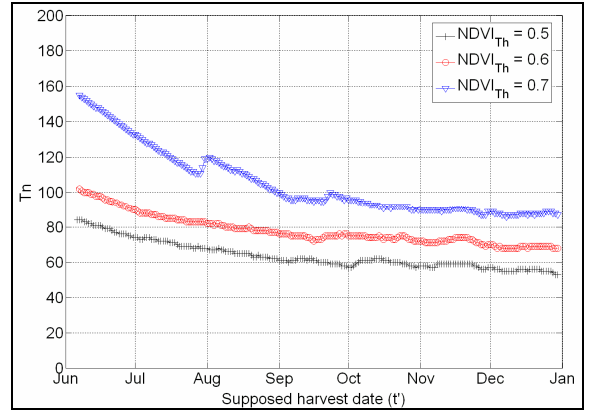


Figure 3. Examples of relationships between the supposed harvest date that relates to the NDVI simulation starting date, which is the acquisition date t' , and the nominal time (T_n) required to reach a given NDVI threshold $NDVI_{Th}$.

In our application, knowledge about the sugarcane cycle, its cropping system, and its phenology were collected from experts to facilitate the harvest detection process.

5 Information fusion in an expert system

To deal with the multi-source information and to make decisions, one must design an appropriate framework that defines the use of each source, characterizes the output, and identifies the information fusion technique.

Because of its well known ability to deal with imprecise and uncertain information, and to model linguistic concepts, fuzzy logic formalism was chosen to design an expert system for the sugarcane harvest detection. The developed system provides decision (harvested or not-harvested) about a sugarcane field between two acquisition dates t and t' .

5.1 System inputs

System inputs consisted of 11 parameters built using information extracted from three different sources: time series of SPOT5 images, crop growth modeling, and expert knowledge.

The first set of inputs (In1, In2, In3, In4 and In5) concerned temporal information, the second set (In6, In7 and In8) related to NDVI values, and the third set (In9, In10 and In11) dealt with NDVI dynamics. A detailed description of these inputs can be found in [19]. Here is a brief overview:

- In1 and In2 are the classes of acquisition dates t and t' respectively.
- In3 compares the temporal distance (in days) between t and the last harvest date with the nominal cycle length of sugarcane.
- In4 compares the temporal distance ($t-t'$) with T_n .
- In5 compares the difference between t and the date of the beginning of the harvest campaign with T_n .

- In6, and In7 are classes of NDVI(t) and NDVI(t') respectively.
- In8 is a qualitative indicator of the amount of t' for which NDVI values (NDVI(t')) are High (t' = all dates before t').
- In9 compares the two-date difference in NDVI calculated at t and t' with a given threshold.
- In10 and In11 check if the sign of the gradient between NDVI(t') and NDVI(t) is negative or positive.

Fuzzy sets and labels were used to define the partitioning of the universe of each input using linguistic concepts. Fuzzy partitioning of In6 and In7 is shown in Figure 4; labels of inputs In1 and In2 are shown in Figure 5; and fuzzy sets of inputs (In3, In4, In5 and In9) are shown in Figure 6. Each of inputs In8, In10 and In11 has four labels: [No t'], [For at least one t'], [For the majority of t'] and [For all t'].

Information from the time series contributed to the definition of all inputs by providing NDVI values or acquisition dates. Expert knowledge was used in the majority of input definitions either by integrating information about the cropping system (nominal cycle length, last harvest date, mill opening and closure dates) or by its role in the configuration of fuzzy input partitions. For example, the NDVI fuzzy sets were designed according to expert knowledge about the phenology and field status of sugarcane as well as about its NDVI temporal profiles. The following are expert conclusions:

- Low NDVI values (< 0.30) generally correspond to residues and bare soil after field harvesting.
- In the growth phase, the NDVI values are Medium (between 0.30 and 0.75). They are also Medium during the senescence phase.
- At the end of the growth stage and before senescence, NDVI values are High (>0.75).

Figure 4 shows the fuzzy sets of NDVI and an example of NDVI profiles plotted according to thermal time for several sugarcane fields.

Information from crop modeling contributed to two key inputs (In4 and In5) that evaluated harvest possibilities by comparing temporal information. An ambiguity range of ±1 month was added to these inputs to account for imprecision of the model and for effects of climatic variation observed for high values of the NDVI threshold.

5.2 Fuzzy rule generation

The rule base of a fuzzy system describes the behavior of the inference based on the linguistic terms associated with the input and output variables. It groups the different possible knowledge-based scenarios by a finite collection of *If X Then Y* rules, e.g.,

Rule 1: if x_1 is A_1^1 and x_2 is A_2^1 ... and x_n is A_n^1 then y is B^1

Rule 2: if x_1 is A_1^2 and x_2 is A_2^2 ... and x_n is A_n^2 then y is B^2

⋮

Rule r: if x_1 is A_1^r and x_2 is A_2^r ... and x_n is A_n^r then y is B^r

(3)

where A_k^r is the fuzzy set of the input variable In k assigned to x_k , and B^r is the conclusion of the r^{th} rule.

The rule base of our system was generated automatically with the software FisPro [20].

Rule generation was based on the construction of a fuzzy decision tree by using a learning dataset. Fuzzy decision trees are an extension of classic decision trees [21, 22]. They are composed of one root and a series of other nodes. Terminal nodes are called leaves. The main advantage of the decision tree is to generate incomplete rules that are only defined by a subset of the available input variables.

The tree induction is an iterative process; at each step, a new node is added. Each node corresponds to a split on the values of one input variable. This variable is chosen to reach a maximum of homogeneity among the examples that belong to the node, relative to the output variable. A node generates a number of sub-nodes equal to the number of fuzzy sets of the selected variable. This is equivalent to minimizing entropy. The paths from the root node toward the leaf nodes are easy to interpret as decision rules [23].

Fuzzy decision trees proposed in FisPro are based on an implementation of the fuzzy ID3 algorithm [24]. The space partitioning of each input must be user-defined prior to running the algorithm.

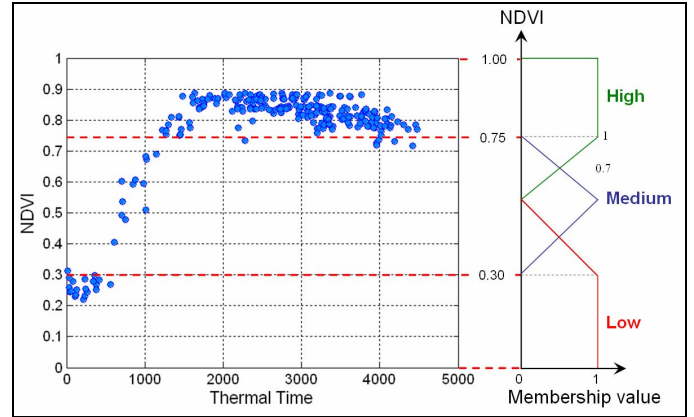


Figure 4. NDVI profiles plotted according to thermal time for several sugarcane fields. On the right are the fuzzy sets of NDVI-defined inputs In6 and In7.

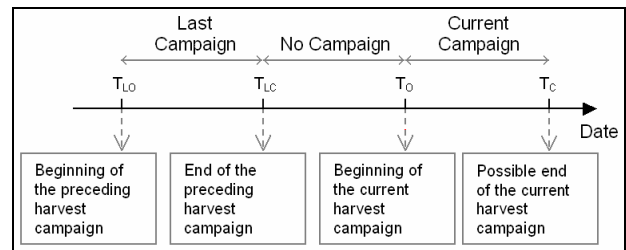


Figure 5. Temporal intervals used for the classification of image acquisition dates. T_{LO} , T_{LC} , T_O and T_C are the beginning and end dates of the last and the current harvest campaign respectively.

5.3 System inference

The generated rules base is used to infer decisions for new input values. The inference method defines the way in which the system attributes weights to the conclusions of the rules that are fired by new input values, and the way it aggregates the weighted conclusions of these rules in order to assign membership degrees to the decision labels. The inference technique used in our expert system is based on Mamdani's method. The weight w^r attributed to the conclusion B^r of an activated rule r is calculated by combining the membership degrees of rule premises in a conjunctive way using the *min* t-norm:

$$w^r(B^r) = \min(\mu_{A_1^r}(x_1), \mu_{A_2^r}(x_2), \dots, \mu_{A_p^r}(x_p)) \quad (4)$$

where $\mu_{A_j^r}(x_j)$ is the membership degree of the x_j value to the fuzzy set A_j^r .

The aggregation of the distinct conclusions of the m activated rules is done in a disjunctive way using the *max* t-norm. Therefore, the membership degree μ_j assigned to the decision label j is calculated as follows:

$$\mu_j = \left\{ \begin{array}{l} \forall j = 1, \dots, m \\ \max_r (w^r(B^r)) \mid B^r = j \end{array} \right\} \quad (5)$$

To obtain a crisp decision, a defuzzification operator that retains the label j with the highest membership degree μ_j is used. Then, the inferred system decision about the status of a sugarcane field between two acquisition dates t and t' for each new set of 11 input values is either harvested or not-harvested.

6 Results

The expert system was used to automatically detect the harvest of sugarcane fields at the study site using the 10 SPOT5 images.

Different percentages of learning data were used for the generation of the system rules. The aim was to evaluate the sensitivity of the system to the variation in the learning dataset size. A learning dataset consisted of input values calculated for a given percentage of sugarcane fields on all acquisition dates with the corresponding status (harvested or not-harvested) available from ground truth data.

Figure 7 shows an example of a rule generated automatically using 50% of the data for training; this rule can be easily interpreted because of the linguistic aspect of the input and the conclusion variables. By interpreting each generated rule we can understand which scenario it reflects, and therefore evaluate its generic aspect.

For each percentage of learning data, the system was used to make decisions for the rest of the fields for all dates. To make a robust evaluation, a k-fold cross-validation, with $k = 10$, was made for each case.

Figure 8 shows the overall accuracy (OA) of the system obtained with different percentages of learning data and after a 10-fold cross-validation.

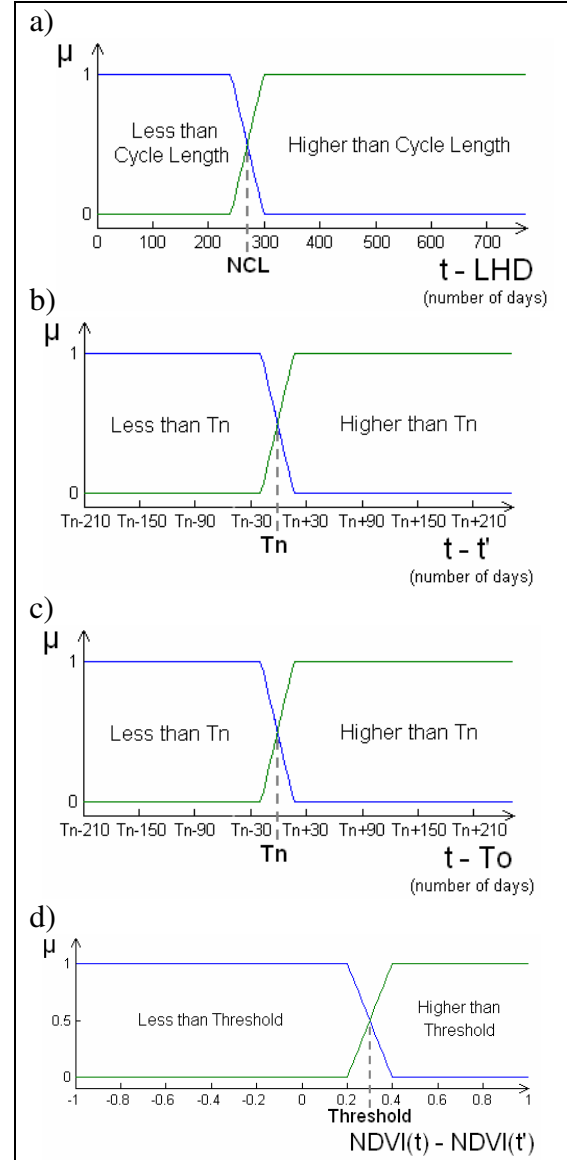


Figure 6. Fuzzy sets of inputs In3 (a), In4 (b), In5 (c) and In9 (d). LHD = Last harvest date; NCL = Nominal cycle length, T_n = Nominal time; and T_o = opening mill date.

It is clear that the system decisions were in substantial agreement with the ground truth data; OA values exceeded 91% in all cases. A very satisfactory OA value of 96.07% was reached when the percentage of learning data was about 50%.

7 Conclusion

This paper presented a novel approach for dealing with time series of optical satellite images used for crop monitoring. Data extracted from time series were combined with information from crop model output and expert knowledge, in order to make credible decisions.

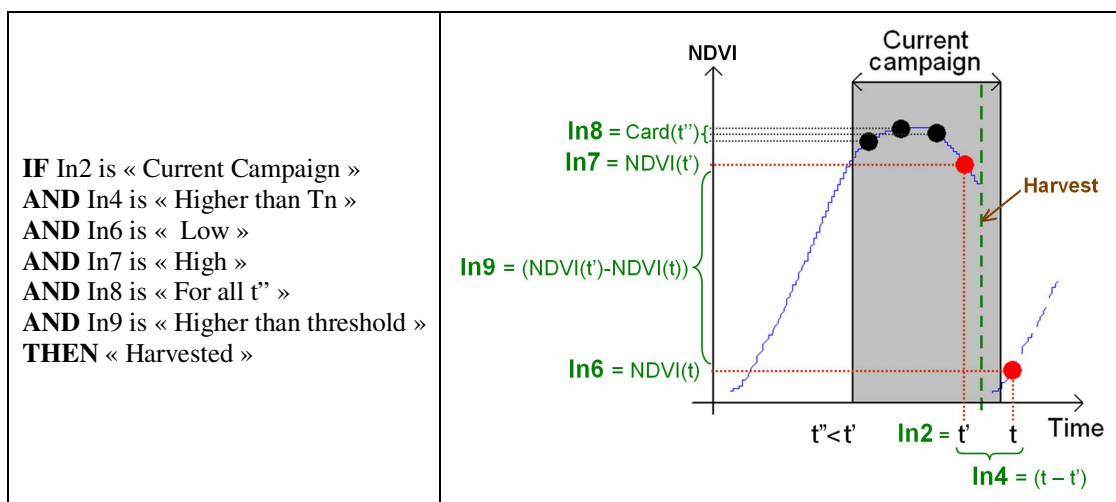


Figure 7. An example of a rule generated automatically using learning data, with a schematisation of the scenario that it reflects. The rule is defined using a subset of input variables (In1, . . . , In11) and a conclusion. Each point in the NDVI temporal profile represents the NDVI value of the sugarcane field calculated at a given acquisition date (t , t' or $t'' < t'$).

The description of the approach was done using an application example of sugarcane harvest monitoring with a SPOT5 time series. An expert system designed and implemented for automatic harvest detection was described.

Results obtained when evaluating the expert system were in substantial agreement with ground truth data; the overall accuracy reached 96.07%. The next step concerning the sugarcane application consists in examining the robustness of the automatically generated rules by testing the system at other sites and in other years. It would also be interesting to analyze the contribution of each information source to system performance.

The approach outlined in this paper is generic and very promising. Many models that simulate the growth of the main annual crops exist (e.g., STICS [25]), and expert knowledge about these crops could be obtained easily either from farmers or from agronomic knowledge bases [26]. The combination of crop model outputs and expert knowledge with time series of high spatial-resolution satellite-images seems to be an excellent tool for crop monitoring.

Acknowledgments

We would like to thank H el ene de Boissezon (CNES) and Thierry Rabaute (C-S) for their help and support. We would also like to thank the CNES for funding the KALIDEOS database (<http://kalideos.cnes.fr>) and for generously providing the SPOT5 images. Mahmoud El Hajj is supported by a Cemagref/R egion Languedoc Roussillon (France) Ph.D. fellowship.

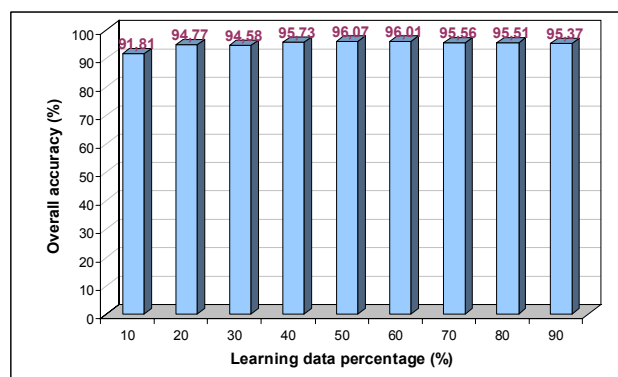


Figure 8. Overall accuracy of the expert system using different percentages of learning data.

References

- [1] M. Pax-Lenney and C. E. Woodcock, "Monitoring agricultural lands in Egypt with multitemporal landsat TM imagery: How many images are needed?," *Remote Sensing of Environment*, vol. 59, pp. 522-529, 1997.
- [2] G. A. Ippoliti-Ramilo, J. C. N. Epiphanyo, and Y. E. Shimabukuro, "Landsat-5 Thematic Mapper data for pre-planting crop area evaluation in tropical countries," *International Journal of Remote Sensing*, vol. 24, pp. 1521-1534, 2003.
- [3] C. S. Murthy, P. V. Raju, and K. V. S. Badrinath, "Classification of wheat crop with multi-temporal images: Performance of maximum likelihood and artificial neural networks," *International Journal of Remote Sensing*, vol. 24, pp. 4871-4890, 2003.
- [4] M. D. Turner and R. G. Congalton, "Classification of multi-temporal SPOT-XS satellite data for mapping rice fields on a West African floodplain,"

- International Journal of Remote Sensing*, vol. 19, pp. 21-41, 1998.
- [5] J. A. Martinez-Casasnovas, A. Martin-Montero, and M. A. Casterad, "Mapping multi-year cropping patterns in small irrigation districts from time-series analysis of Landsat TM images," *European Journal of Agronomy*, vol. 23, pp. 159-169, 2005.
- [6] S. Panigrahy and S. A. Sharma, "Mapping of crop rotation using multirate Indian Remote Sensing Satellite digital data," *ISPRS Journal of Photogrammetry and Remote Sensing*, vol. 52, pp. 85-91, 1997.
- [7] L. Bruzzone and P. Smits, "Analysis of Multi-temporal Remote Sensing Images : Multitemp 2001," in *Series in remote sensing*, vol. 2, A. P. Cracknell, Ed.: World Scientific Publishing Co. Pte. Ltd., 2002, pp. 440.
- [8] P. Smits and L. Bruzzone, "Analysis of Multi-temporal Remote Sensing Images : MultiTemp 2003," in *Series in remote sensing*, vol. 3, A. P. Cracknell, Ed.: World Scientific Publishing Co. Pte. Ltd., 2004, pp. 387.
- [9] R. Lucas, A. Rowlands, A. Brown, S. Keyworth, and P. Bunting, "Rule-based classification of multi-temporal satellite imagery for habitat and agricultural land cover mapping," *Isprs Journal of Photogrammetry and Remote Sensing*, vol. 62, pp. 165-185, 2007.
- [10] G. Metternicht, "Assessing temporal and spatial changes of salinity using fuzzy logic, remote sensing and GIS. Foundations of an expert system," *Ecological Modelling*, vol. 144, pp. 163-179, 2001.
- [11] S. Le Hegarat-Masclé, R. Seltz, L. Hubert-Moy, S. Corgne, and N. Stach, "Performance of change detection using remotely sensed data and evidential fusion: Comparison of three cases of application," *International Journal of Remote Sensing*, vol. 27, pp. 3515-3532, 2006.
- [12] S. Moulin, A. Bondeau, and R. Delécolle, "Combining agricultural crop models and satellite observations: From field to regional scales," *International Journal of Remote Sensing*, vol. 19, pp. 1021-1036, 1998.
- [13] H. DeBoissezon and A. Sand, "Reference Remote Sensing Data Bases: Temporal series of calibrated and ortho-rectified satellite images for scientific use," presented at Proceedings of Recent Advances in Quantitative Remote Sensing, Valencia, Spain, 2006.
- [14] <http://kalideos.cnes.fr>, "Images Spot: copyright CNES, Distribution Spot Image," 2007.
- [15] M. El Hajj, A. Bégué, B. Lafrance, O. Hagolle, G. Dedieu, and M. Rumeau, "Relative radiometric normalization and atmospheric correction of a SPOT 5 time series," *Sensors*, vol. 8, pp. 2774-2791, 2008.
- [16] M. El Hajj, M. Rumeau, A. Bégué, O. Hagolle, and G. Dedieu, "Radiometric normalization of high spatial resolution multi-temporal imagery: A comparison between a relative method and atmospheric correction," presented at Proceedings of SPIE Europe Remote Sensing - The International Society for Optical Engineering, Florence, Italy, 2007.
- [17] A. Bégué, "Leaf area index, intercepted photosynthetically active radiation, and spectral vegetation indices: a sensitivity analysis for regular-clumped canopies," *Remote Sensing of Environment*, vol. 46, pp. 45-59, 1993.
- [18] J. F. Martiné and P. Todoroff, "Le modèle de croissance Mosicas et sa plateforme de simulation Simulex: état des lieux et perspectives," *Revue Agricole et Sucrière de l'île Maurice*, vol. 81, pp. 133-147, 2002.
- [19] M. El Hajj, A. Bégué, and S. Guillaume, "Multi-source information fusion: Monitoring sugarcane harvest using multi-temporal images, crop growth modelling, and expert knowledge," presented at MULTITEMP-2007, Fourth International Workshop on the Analysis of Multi-Temporal Remote Sensing Images, Provinciehuis Leuven, Belgium, 2007.
- [20] S. Guillaume, B. Charnomordic, and J.-L. Lablée, "FisPro: Logiciel open source pour les systèmes d'inférence floue," <http://www.inra.fr/bia/M/fispro>, Ed.: INRA-Cemagref, 2002.
- [21] L. Breiman, J. H. Friedman, R. A. Olshen, and C. J. Stone, *Classification and Regression Trees*. Belmont CA, 1984.
- [22] J. R. Quinlan, "Induction of decision trees," *Machine Learning*, vol. 1, pp. 81-106, 1986.
- [23] S. Guillaume, "Designing Fuzzy Inference Systems from Data: An Interpretability-Oriented Review," *IEEE Transactions on Fuzzy Systems*, vol. 9, 2001.
- [24] H. Ichihashi, T. Shirai, K. Nagasaka, and T. Miyoshi, "Neuro-fuzzy ID3: A method of inducing fuzzy decision trees with linear programming for maximizing entropy and an algebraic method for incremental learning," *Fuzzy Sets and Systems*, vol. 81, pp. 157-167, 1996.
- [25] INRA, "STICS : Simulateur multIdisciplinaire pour les Cultures Standard," <http://www.avignon.inra.fr/stics/>.
- [26] G. Russell, R. I. Muetzelfeldt, K. Taylor, and J. M. Terres, "Development of a crop knowledge base for Europe," *European Journal of Agronomy*, vol. 11, pp. 187-206, 1999.